Research Journal of Applied Sciences, Engineering and Technology 8(11): 1340-1349, 2014
DOI:10.19026/rjaset.8.1105
ISSN: 2040-7459; e-ISSN: 2040-7467

Submitted: May 31, 2014 Accepted: July 13, 2014 Published: September 20, 2014

Research Article

Sparse Space Replica Based Image Reconstruction via Cartesian and Spiral Sampling Strategies

[1]K.L. Nisha, [2]B. Shaji and [3]N.R. Rammohan
[1]Department of Electronics and Communication and Engineering, Arunachala College of Engineering for Woman,
[2]Department of Information Technology, Marthandam College of Engineering and Technology,
[3]Department of Computer Science and Engineering, Sun College of Engineering and Technology, Nagercoil, Tamilnadu, India

Abstract: In this study, a replica based image reconstruction is designed to provide high-quality reconstructions from very sparse space data. The problem of reconstructing an image from its unequal frequency samples take place in many applications. Images are observed on a spherical manifold, where one seeks to get an improved unidentified image from linear capacity, which is noisy, imperfect through a convolution procedure. Existing framework for Total Variation (TV) inpainting on the sphere includes fast methods to render the inpainting problem computationally practicable at high-resolution. In recent times, a new sampling theorem on the sphere developed, reduces the necessary number of samples by a feature of two for equiangular sampling schemes but the image that is not extremely sparse in its gradient. Total Variation (TV) inpainting fails to recover signals in the spatial domain directly with improved dimensionality signal. The regularization behavior is explained by using the theory of Lagrangian multiplier but space limitation fails to discover effective connection. To overcome these issues, Replica based Image Reconstruction (RIR) is developed in this study. RIR presents reconstruction results using both Cartesian and spiral sampling strategies using data simulated from a real acquisition to improved dimensionality signal in the spatial domain directly. RIR combined with the Global Reconstruction Constraint to remove the noisy imperfect area and highly sparse in its gradient. The proposed RIR method leads to significant improvements in SNR with very sparse space for effective analytical connection result. Moreover, the gain in SNR is traded for fewer space samples. Experimental evaluation is performed on the fMRI Data Set for Visual Image Reconstruction. RIR method performance is compared against the exiting TV framework in terms of execution time, Noisy area in SNR, accuracy rate, computational complexity, mean relative error and image dimensionality enhancement.

Keywords: Cartesian, dimensionality signal, frequency samples, global constraint, replica based image reconstruction, sparse data, spiral sampling strategies, total variation method

INTRODUCTION

In most image reconstruction problems, the images are not openly visible. Instead, one scrutinizes a transformed version of the image, probably corrupted by noise. In the common case, the estimation of the image is regard as a concurrent de-convolution and de-noising problem. Automatically, a better reconstruction is get hold of it by incorporating information of the image into the reconstruction algorithm. Dynamic imaging is a significant and rapidly mounting area with profound implications for medical diagnosis and treatment. Hexagonal images spend the hexagonal Fourier transform by Koo and Cho (2011) which involves image sampling on a hexagonal lattice follow by a normalized hexagonal cross-correlation in the frequency domain. The term sub-pixel is defined on a hexagonal grid in order to attain floating point register. Artificially induced motion and actual motion reveal the frequency-domain motion estimation on a square lattice, in the shape of phase correlation.

Many images arising in medical imaging applications consist of numerous regions in which the pixel values are constant. A similar edge-enhancing operation transforms the image reconstruction difficulty into one of reconstructing relatively with few non-zero pixel values. Edge enhancing operation requires a much lesser quantity of data values and result in a much smaller-sized problem than reconstructing the entire image from many more pixel values. Spatial Sparsity-Induced Prediction (SIP) fails to incorporate tracking algorithms by Babacan *et al*. (2011) to track targets in complex scenes within vision algorithms to intelligently

Corresponding Author: K.L. Nisha, Department of Electronics and Communication and Engineering, Arunachala College of Engineering for Woman, Tamilnadu, India

segment and analyze such scenes within medical registration algorithms.

Gaussian Markov random Field (MRF) is effective system as expressed by Li (2011) and Hu *et al*. (2011) estimated a spatially high-resolution image from specified multiple low-resolution images. Inhomogeneous Gaussian Markov Random Field (IGMRF) predictable using the same preliminary HR estimate. Point estimates such as MAP and ML are generally not stable in ill-posed high-dimensional problems because of over fitting, while PM is a stable estimator because all the parameters in the model are evaluated as distributions. The estimator is numerically determined by using variation Bayes. The conjugate prior problem in variation Bayes introduces three Taylor approximations to achieve maximum likelihood.

Nontrivial prediction scenarios involve images and video frames where statistically connected data is rendered unproductive for conventional methods due to cross-fades, blends, clutter, brightness variations, focus changes and other complex transitions. Non-negative matrix factorization algorithm as described by Lefkimmiatis *et al*. (2011) which divide fluorescent images into true signal and Auto Fluorescence (AF) components. An AF component utilizes an estimate of the dark current for complex transitions.

Sparse images emerge obviously, for example, in radio astronomy and molecular imaging. As well, a non-sparse image might have a sparse representation in several suitable domains. For illustration, an image collected of abundant constant-valued areas will, ahead spatial separation, become sparse. The model where the surveillance is a linear change of the image is degraded by additive white Gaussian noise. There are numerous existing methods that tackle the sparse image reconstruction problem. Reconstruction algorithms naturally depend on a set of parameters that need to adjust properly for obtaining good image-quality. Deciding the suitable parameter values is a nontrivial, application dependent task and has provoked investigate on automated parameter selection based on quantitative measures.

The compressed sensing image recovery problem using adaptive nonlinear filtering strategies as illustrated by Afonso *et al*. (2011) provided evidence of the resulting two-steps iterative scheme. Acquisition matrix is obtained as randomly chosen rows of an orthogonal transform, the two steps of the iterative procedure turn out to be an enforcing of the present iterate with the specified measurements. The results of experiments authenticate that the corresponding algorithm possesses the required properties of efficiency, stability and its performance is competitive with those of the state of the art algorithms.

Image-specific and region-specific linear as demonstrated by Chen *et al*. (2011) strengthened filter response also be controlled in order to transfer the structural information of a channel to the others. Image fusion and chrominance image interpolation with de-noising prove that MAP-MRF formulation offer improved subjective and objective performance with conventional approaches. Gaussian components (classes) as expressed by Shi *et al*. (2011), initially considered each dishonored frame and the variety of the optimal number of classes according to the global relative entropy criterion. The iterative application of classification and fusion, go behind by optimal adaptive filtering, unite to a global enhanced representation of the original scene. In these cases, dynamically varying models uses selection of the optimal number. The optimal number of Gaussian components performed based upon the Akaike Information Criterion (AIC).

Pyramid Beam (PB) as expressed by Montefusco *et al*. (2011) is based upon the parallel reconstruction algorithm that allow fast capturing of the scanned data and in 3-D, the reconstructions are based upon the discrete X-ray transform. The PB geometries are rearranged to fit parallel projection geometry. The underlying idea is to use the PB geometries. Optimization reconstruction stage by Gajjar and Joshi (2010) is computed by different models according to the prior knowledge of scenes. The imaging method offers a new way of acquiring HR images of fundamentally static scenes when the camera resolution is imperfect by severe constraints.

Iterative Reweighted Least Squares (IRLS) type by Katsuki *et al*. (2012) resulted from a majorization-minimization approach relies on a dilemma specific Preconditioned Conjugate Gradient method (PCG). IRLS makes the overall minimization scheme very attractive because it professionally applied to huge images in reasonable time. Minimization of penalized least squares criterion in the circumstance of image restoration, using the subspace algorithm approach. An innovative multidimensional search policy based on majorize-minimize principle demonstrated by Argyriou (2011) leads to a closed-form step size procedure. Procedure ensures the convergence of the subspace algorithm bit within the limited space.

In this study, focus is made on Replica based Image Reconstruction (RIR) which results in the significant improvements in SNR with higher resolutions in space. The RIR method with Global Reconstruction Constraint has the benefit of computational complexity. RIR used prior information in the form of a replica model during perfusion. In this way, the reconstruction task is minimized by estimating every pixel intensity over time that approximates only the replicas of the model. As a result, replica based reconstruction mechanism leads to significant enhancement in SNR. Additionally, the gain in SNR with fewer space samples, lead to acquisitions with higher resolutions in space.

MATERIALS AND METHODS

The idea behind RIR method is to get the low frequency components in each time frame via the central sparse space curves, while making the high-

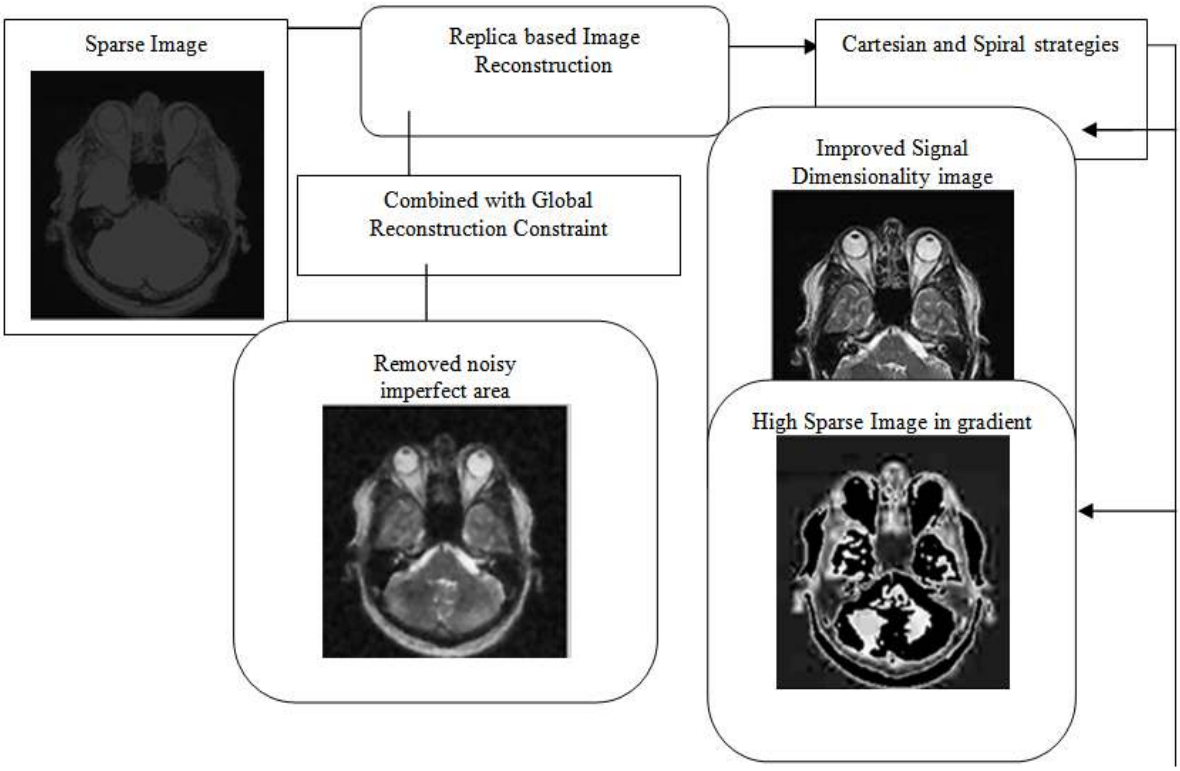

Fig. 1: Diagrammatic flow of replica based image reconstruction

frequency errors across time frames as independent as possible. The space sample is to sample spiral lines, along the interpret direction, that follow a specific pattern. The strategies in the RIR method significantly differ from conventional ones. Reconstructions from non-Cartesian space sampling to spiral sampling entail modifications to the Cartesian parallel imaging in RIR method. The below Fig. 1 illustrate the diagrammatic flow of replica based image reconstruction.

Figure 1 describes the overall framework replica based image reconstruction. Sparse image has pixel values that are typically zero, with a minute quantity of nonzero values at un-known locations. The number of known values must go beyond four times the number of nonzero pixel values. Replica based reconstruction reduce the reconstruction task from estimating each pixel intensity over time to estimating only the constraint of the model. RIR combined with the global constraints profitably applied in de-noising and imperfect area removal. These connections make available context for additional improving the performance, at the cost of decreased computational complexity Replica based on constraints encodes stronger prior information and, hence, have the ability to produce superior result. Cartesian and spiral strategies on time frame from sparse space data sampled to retain more information from the imaged signal with improved signal dimensionality and higher sparse in gradient.

Mathematical model of RIR method: Represent the amount at pixel 'p' and instance't' in the reconstruct image series with the function $f(\alpha, p, t)$ to denote the complete series of reconstructed images. Let us indicate the specified sparse space image as i (p, t). The Fourier F (*) and Inverse Fourier transform F^{-1} (*) denote the reduction operator R (*) that zeros out those elements from the sparse space where the image is not provided. Then define energy of the structure with spiral strategies that quantifies the discrepancy between the estimated image reconstructions and the data:

$$E(\propto) = |RFf(\propto) - i|^2 \quad (1)$$

In a regular inverse methods formulation, the task is to find image reconstructions with cartesian and spiral strategies of f(α), such that α would produce sparse space image as close to the given image 'i', thereby minimizing the energy $E(\propto)$:

$$\propto^{utmost} = min_{\propto} E(\propto) \quad (2)$$

$\propto^{utmost}$ Contains the complete information about the sparse image energy, $min_{\propto}$ chooses the minimum energy used for RIR processing. RIR employ an iterative gradient descent optimization strategy, with restricted forward differences. An estimation of the parameter $\propto^n$ at iteration 'n' define:

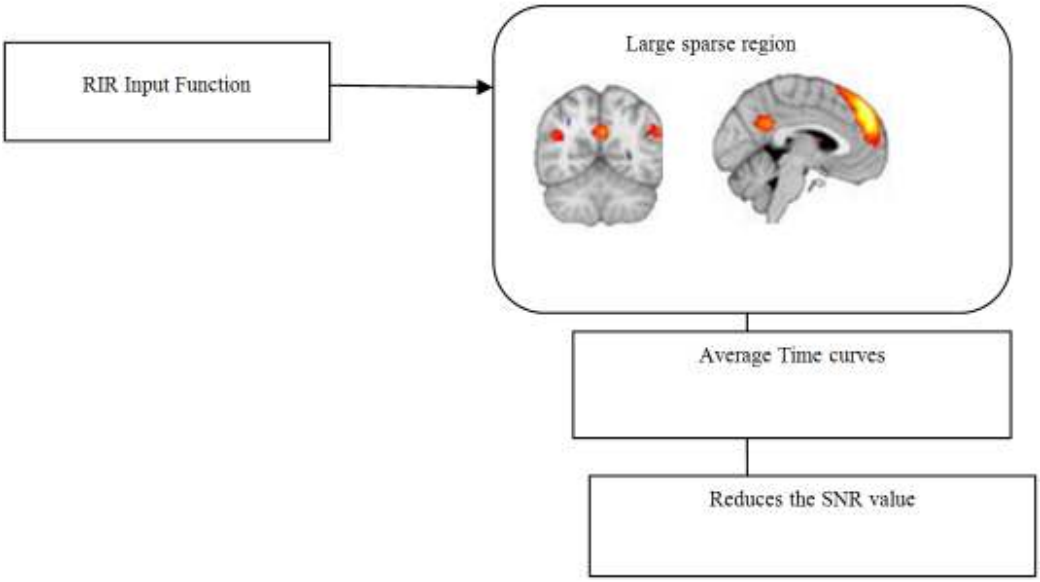

Fig. 2: Input function of RIR

$$\propto^{n+1} = \propto^{n} - \omega \frac{\partial E(\propto)}{\partial \propto}$$

$$= \propto^{n} - \omega \frac{\partial E(\propto)}{\partial f} \frac{\partial f(\propto)}{\partial \propto} \quad (3)$$

where, ω is the update rate, $\partial E(\propto)$ is the energy consumed on the image '$\propto'$ to the total image group $\partial \propto$. As the iterations passes, obtains the estimated function:

$$\frac{\partial E(\propto)}{\partial f} = 2[F^{-1}(RF_f(\propto) - i)] \quad (4)$$

The inverse value of energy consumption is obtained with the reduction operator 'R' and Fourier transform function 'F_f' produce sparse space image $\propto$ as different to the given image 'i'. RIR method with global constraint does not hold significant expressive power and get rid of inappropriate data accurately. Spiral form in RIR is the curve which emanates to improve the dimensionality signal. For minimalism of computations in RIR method, presuppose the phase ∅(p) to be zero at all pixels point of the spiral and Cartesian strategy images.

Global reconstruction constraint in replica method: The accurate impartiality between the global reconstructions constraint used to highly sparse in gradient. The trouble-free global constraint viewed as a special case of a general sparse representation framework for inverse Fourier transform in image processing. These connections provide context for understanding work and also suggest means of decreasing computational complexity. Given sufficient computational resources, RIR principle solve for the coefficients associated with all patches simultaneously. In addition, RIR with global constraint contain complete high frequency images 'I' as a variable.

Relatively demanding that 'I' be completely reproduces by the sparse coefficients, penalize the dissimilarity among 'I" and the high frequency image. High resolution given by these coefficients allows solutions that are not completely sparse, but enhanced assure the reconstruction constraints. RIR with global constraint leads to a large optimization problem with higher sparse rate.

$$I^{*} = \min \sum_{i,j} | \propto_{i,j} | + \rho |I| + \sum_{i,j} |P_{i,j} I|^2 \quad (5)$$

In Eq. (5), $\propto_{i,j}$ denotes the representation coefficients for the (i, j) patch of I and $P_{i,j}$ is a ridge matrix that selects the (i, j) patch from I. ρ (I) is a penalty function that encodes prior knowledge about the image. The function depends on the image category form of a Cartesian and spiral regularization term.

Input/output function of replica based image reconstruction: RIR derive input function (S (t)) from the complete sparse space acquisition. Such groups to provide accurate input functions free from saturation effects. The key idea is that the input function is used to replica everything in the field of view.

Figure 2 contains the replica based image reconstruction input function. The input contain large sparse region with the fMRI Data Set images. These images takes the lesser time curves which leads to the minimal signal to noise ratio. Moreover, the input function has a superior SNR because it is a standard of the time curves taken from a fairly large spatial sparse region.

The replica based image reconstruction output function needs an initial approximation. A gradient descent process is prone to local minima and hence, it is

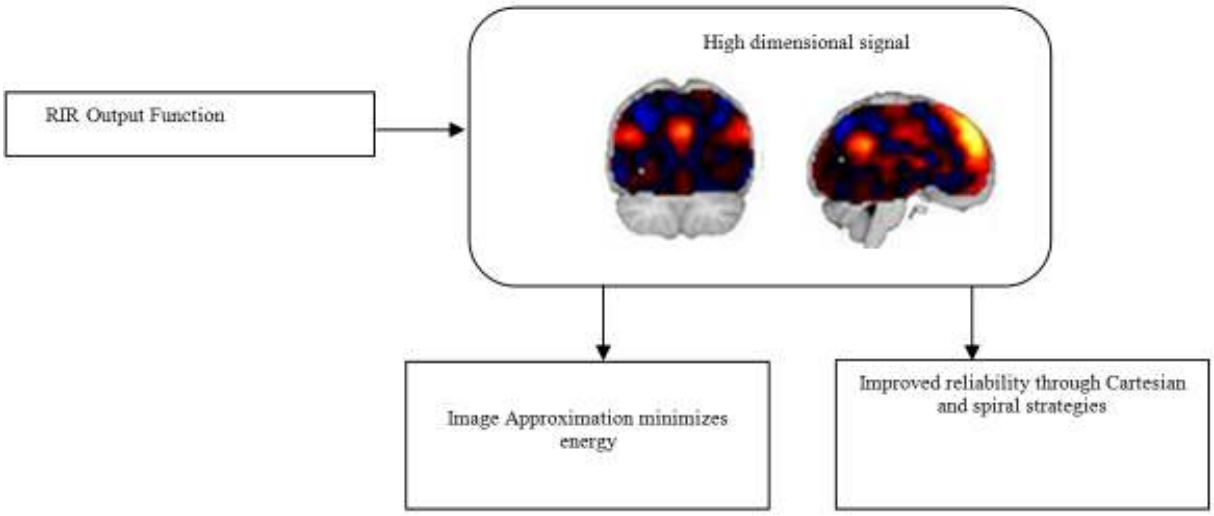

Fig. 3: Output function of RIR

reasonable using an initial approximation that is close to the solution. RIR obtain such an initial approximation by leveraging any current state of the art TV framework. The initial image approximation minimizes an energy which is the sum of a reliability term and a Cartesian and spiral regularization form. The consequence on the chronological gradient of the solution and that implement smoothness on the reconstruct time curves.

Figure 3 provides the output function of the RIR, which produces the result with the improved reliability rate. The former information that incorporates the contrast agent starts only after the few time and, thus, the first few images detain the same signal, which improves the dimensionality rate. The algorithmic flow of the RIR with global constraint is described as:

Begin:
Input: Sparse space data i (p, t)
Output: Reconstruction proceeds with high dimensionality
ForEach 'i' image from fMRI dataset
1: Initial approximation of parameter 'α' obtained
2: Estimate$\propto^n$ at iteration 'n' times
3: Compute constraint approximation $\propto^{n+1}$ via a gradient descent scheme to minimize energy
4: Compute $\frac{\partial E(\propto)}{\partial f} = 2[F^{-1}(RF_f(\propto) - i)]$
End ForEach
End

The replica based image reconstruction assumes that the series of images is well registered and has no motion objects. Here well registered images using complete space information from fMRI Data Set images. RIR apply an inverse-Fourier transform to these images and then take the magnitude of the resulting complex number at each pixel. RIR essentially gives us a reconstruction using complete space data that necessarily well registered time frames. To enforce checking, pixel wise replica, make smoothness over the time curves enforced and produce integral high dimensional images.

RESULTS AND DISCUSSION

Replica based Image Reconstruction (RIR) with the Global Reconstruction Constraint is implemented using MATLAB code. RIR scheme and existing Total Variation (TV) framework uses the fMRI Data Set for Visual Image Reconstruction. fMRI Data Set for Visual Image Reconstruction used custom made machine learning algorithm to train the decoders of multiple scales and shared them based on a trouble-free linear model. The method works very well to renovate visual images from fMRI activity pattern with high accuracy in RIR method. The data set contains preprocessed fMRI data with the corresponding labels (stimulus). The visual stimuli used to train the reconstruction model on arbitrary image patterns, which are unbiased toward any definite spatial patterns.

In the sense, the experiment performed is very comparable to that of accessible field identification using white noise patterns. Beside visual image reconstruction, the data are used for different purposes such as identification of receptive field of human visual cortex, investigation of spatial linearity of dimensionality signals. Experimental evaluation of RIR method and exiting TV framework is performed on the fMRI Data Set for Visual Image Reconstruction. Sparse Image reconstruction using sampling method and replica based reconstruction experimental result on the sparse gradient is shown in Fig. 4.

Figure 4a illustrates the lesser sparse image gradient due to the general and is trivially extended to other sparsity which incorporate localized information.

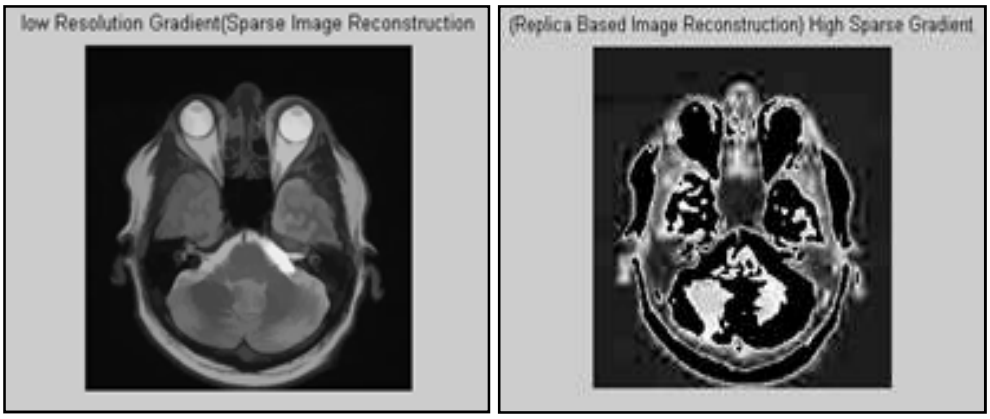

(a) (b)

Fig. 4: Experimental images on low and high sparse gradient

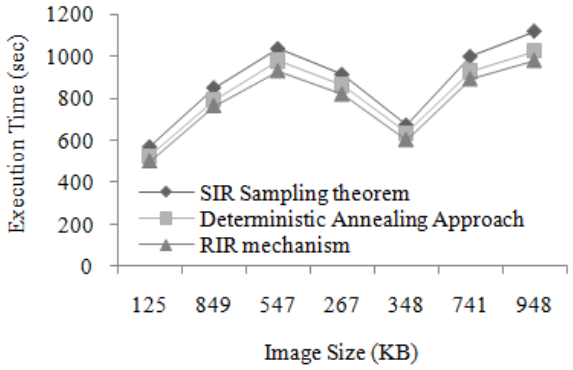

Fig. 5: Performance of execution time

Table 1: Tabulation of execution time

	Execution time (sec)		
Image size (KB)	SIR sampling theorem	Deterministic annealing approach	RIR mechanism
125	570	525	500
849	850	792	765
547	1035	978	930
267	913	862	819
348	673	632	602
741	998	927	892
948	1118	1023	981

In Replica based Image Reconstruction (RIR) obtains the higher sparse gradient using both Cartesian and spiral sampling strategies. RIR mechanism assumes that the sequence of fMRI Data Set images with constraint approximation $\propto^{n+1}$ incorporate registration into the proposed reconstruction scheme, to attain higher sparse image.

Replica based Image Reconstruction (RIR) mechanism is compared against the existing Sparse Image Reconstruction (SIR) via sampling theorem and Deterministic Annealing (DA) based approach toward spatial adaptation in projection-based image de-blurring. An experiment with execution time factor is defined as the time taken to improve signal dimensional image and execute the RIR system. SNR factor is that compares the level of a desired signal to the level of background noise in sparse image. Noisy area in SNR is defined as the ratio of signal power to the noise power, expressed in decibels. A ratio lesser than 0 dB, indicates lesser noise in sparse image.

Image reconstruction accuracy rate is expressed as high quality resolution classifier with maximum likelihood, measured in terms of Kilo bits per second (Kbps). Computational complexity factor is focuses on classifying computational problems according to their intrinsic complexity and connecting those classes to each other for reducing complexity. Mean relative error in RIR I s measured as the quantity used to measure how close predictions take place to obtain effective quality image outcomes, measured in error percentage. Image dimensionality factor is used in result analysis to reducing the number of random variables under enhancement process, measured in terms of pixels. The below evaluation table and graph describes the RIR mechanism against the existing system.

Table 1 describes the execution time factor values of SIR Sampling theorem, Deterministic Annealing Approach and RIR mechanism.

Figure 5 demonstrates the execution time based on the fMRI image size form UCI repository. The execution time of RIR is 10-14% less when compared with the SIR Sampling theorem (Giannoula, 2011) because initial image approximation minimizes an execution time with the sum of a reliability term and a Cartesian and spiral regularization form. The consequence on the chronological gradient of the solution and that implement smoothness on the reconstruct time curves, still reduces the execution time by 3-7% in RIR when compared with Deterministic Annealing Approach (Averbuch *et al*., 2011).

Table 2: Noise area in SNR tabulation

	Noise area in SNR (dB)		
Images	SIR sampling theorem	Deterministic annealing approach	RIR mechanism
Image_ fMRI_1	0.0097	0.0085	0.0080
Image_ fMRI_2	0.0084	0.00704	0.0070
Image_ fMRI_3	0.0099	0.0087	0.0081
Image_ fMRI_4	0.0071	0.0062	0.0057
Image_ fMRI_5	0.0053	0.0047	0.0043
Image_ fMRI_6	0.0061	0.0054	0.0050
Image_ fMRI_7	0.0092	0.0081	0.0076

Table 3: Tabulation of accuracy rate

	Accuracy rate (Kbps)		
Iterations	SIR sampling theorem	Deterministic annealing approach	RIR mechanism
1	1200	1255	1350
2	1230	1310	1380
3	1670	1750	1895
4	1485	1535	1665
5	1400	1515	1640
6	1985	2185	2310
7	1340	1395	1510

Table 4: Tabulation of computational complexity

	Computational complexity (%)		
Image pixels count	SIR sampling theorem	Deterministic annealing approach	RIR mechanism
100	6	5	4
200	16	14	12
300	42	33	30
400	22	19	16
500	6	5	4
600	8	7	6
700	16	14	12

Table 5: Mean relative error measurement

	Mean relative error (Error %)		
Bit per pixel (bpp)	SIR sampling theorem	Deterministic annealing approach	RIR mechanism
25	7.04	6.53	6.19
50	10.13	9.78	9.09
75	9.57	8.95	8.45
100	11.19	10.23	9.85
125	16.55	15.26	14.89
150	14.46	13.16	12.46
175	27.71	25.14	24.27

Table 6: Tabulation of image dimensionality measure

	Image dimensionality enhancement (pixels)		
Image rate (Kbps)	SIR sampling theorem	Deterministic annealing approach	RIR mechanism
1000	715	727	820
1300	552	559	654
1600	821	870	965
1900	491	512	592
2200	515	552	623
2500	370	375	447
2800	635	668	747
3100	743	786	869

Table 2 describes the noise area present in SNR and measured for SIR Sampling theorem, Deterministic Annealing Approach and RIR mechanism.

Figure 6 describes the noise area in SNR measure based on the different image experimentation. The number of known values must go beyond four times the number of nonzero pixel values. RIR combined with the global constraints profitably applied in de-noising and imperfect area removal. The noise area is reduced in RIR mechanism to about 16-19% when compared with the SIR Sampling theorem and 7-10% reduced when compared with Deterministic Annealing Approach (Giannoula, 2011; Averbuch *et al*., 2011). Replica based reconstruction reduce the reconstruction task from estimating each pixel intensity over time to estimate the constraint of the mechanism.

Table 3 and Fig. 7 illustrate the accuracy rate based on the iteration count. As the iterations conducted using fMRI dataset, results are acquired to perform the result analysis. Accuracy rate in RIR mechanism apply inverse-Fourier transform to fMRI images and attain 12-18% improved result when compared with SIR Sampling theorem (Giannoula, 2011). RIR mechanism is also improved to 5-9% when compared with the Deterministic Annealing Approach (Averbuch *et al*., 2011). Inverse-Fourier transform take the magnitude of the resulting complex number at each pixel.

Table 4 and Fig. 8 describe the computational complexity based on the pixel count of fMRI image. As the pixel count get increased, computational complexity is computed to represent through graph. In a RIR regular inverse methods formulation, the task is to find image reconstructions with cartesian and spiral strategies of f (α), such that α would produce sparse space image as close to the given image 'i'. Sparse space images close to image 'i' additional improving the performance with decreased computational complexity. RIR mechanism is 25-33% lesser in complexity when experimented with SIR Sampling theorem and 10-20% when experimented with Deterministic Annealing Approach.

Table 5 and Fig. 9 describe the mean relative error based on the bits per pixel (bpp). Mean relative error is reduced in RIR mechanism with global constraint leads to a large optimization of higher sparse rate. RIR is 10-14% reduces the error rate when compared with SIR Sampling theorem and 2-8% reduced mean error rate when judge against Deterministic Annealing Approach. Eq. (5) in RIR computed to identify the errors and to minimize the error count with prior knowledge about the image. Penalty function is also used as image category form for Cartesian and spiral regularization term separation.

Table 6 illustrates the throughput measure based on the simulation seconds. The Each simulation time

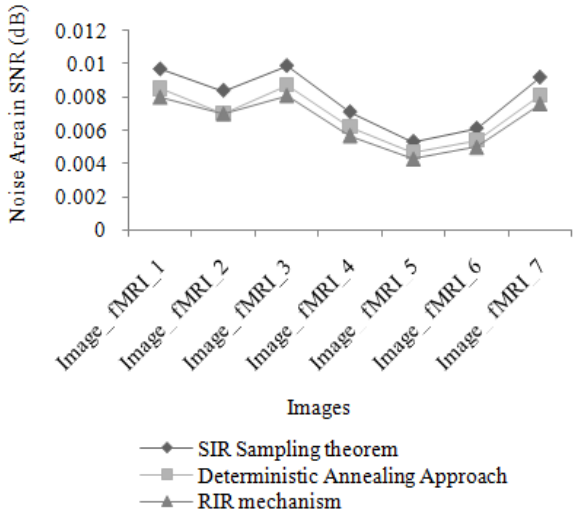

Fig. 6: Noise area in SNR measure

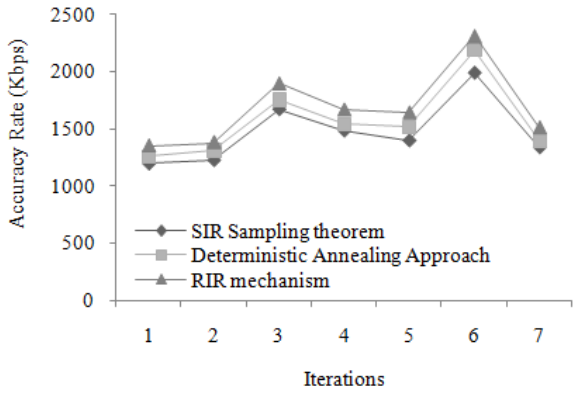

Fig. 7: Performance of accuracy rate

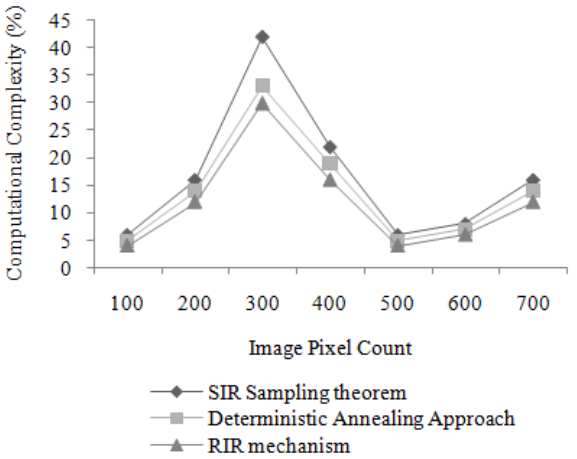

Fig. 8: Computational complexity measure

varies 30 sec. Simulation starts from 100 and depending on count, throughput is measured in LCSAD framework, CMS model and ADD framework.

Figure 10 depicts the image dimensionality based on the image rate. The image rate is measured in terms

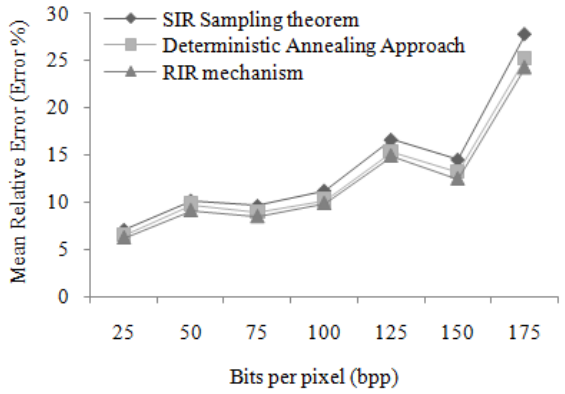

Fig. 9: Mean relative error measure

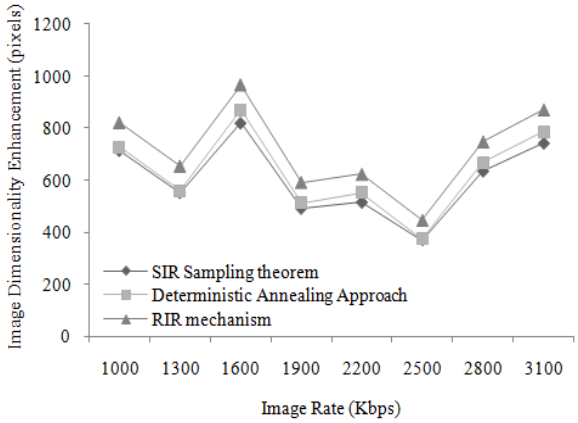

Fig. 10: Measure of image dimensionality

of Kilo bits per second (kbps). Cartesian and spiral strategies on time frame from sparse space data sampled to retain more information from the imaged signal with improved signal dimensionality. RIR improves image dimensionality to 14-20% when compared with SIR Sampling theorem and 10-16% improved when compared with Deterministic Annealing Approach.

RIR mechanism obtains the well registered results from fMRI images. Inverse-Fourier transforms to given image then take the magnitude of the resulting complex number at each pixel. RIR essentially gives us a reconstruction using to magnitude data. The smoothness over the time curves enforces the replica mechanism for generating fitted high sparse images. To facilitate the analysis, RIR mechanism precedes with high quality dimensionality images and reduces the noise ratio level.

LITERATURE REVIEW

A deeper understanding about different regularization filters has only limited space with fine-granularity and spatially adaptive regularization. Similarity transformation and to Blur using orthogonal zernike moments as depicted by Chouzenoux *et al*.

(2011) derive the Zernike moments of a blurred image and the way to construct the combined geometric-blur invariants. PSF is circularly symmetric for a choice happening in real situations. Iterative Shrinkage Approach as illustrated by Liao and Ng (2011) performs de-blurring of digital images corrupted by Poisson noise. The shrinkage approach is derived underneath the supposition that the image of attention sparsely represented in the area of a linear transform. As a result, shrinkage based iterative procedure guarantees the answer to unite global maximize of an associated a posteriori criterion.

Alternating direction method of multipliers one class as shown by Hua and Guleryuz (2011) of constrained problems tailored to image recovery applications. The algorithm, belongs to the family of augmented Lagrangian methods, deal with a variety of imaging. Ill-posed linear inverse problems includes de-convolution and reconstruction from compressive explanation using either total-variation or wavelet-based regularization.

Lagrangian multiplier class of regularization strategy as described by Averbuch *et al*. (2011) is based on the surveillance that a variety of regularized filters vision as non expansive mappings in the metric space. Total Variation (TV)-based blind de-convolution as illustrated by Woolfe *et al*. (2011) estimate both the unknown image and blur estimated within an irregular minimization framework. With the Generalized Cross-Validation (GCV) method, the regularization parameters connected with the unknown image and blur updated in alternating minimization steps. GCV methods for estimation obtain regularization parameters without approximation when compared with Bayesian blind de-convolution algorithms.

Bayesian formulation as demonstrated by Shaked and Michailovich (2011) during the inclusion of uncertainty estimates the algorithms by preventing the propagation of errors among the estimates of a variety of unknowns. Bayesian algorithms are robust to errors in the estimation of only the motion limitation and organized algorithms concurrently to approximate all algorithmic parameters all along with the HR image. Total Variation (TV) inpainting on the sphere as shown by Giannoula (2011), includes fast methods to turn into the inpainting problem computationally feasible at high-resolution but TV does not recover signals in the spatial domain directly.

Local Pixel Structure to Global Image Super-resolution (LPS-GIS) as described by McEwen *et al*. (2013) uses the input Low-Resolution (LR) face image to search a face database for comparable example High-Resolution (HR) faces in order to find out the local pixel structures for the target HR face. It then uses the input LR face and the learned pixel structures as priors to estimate the target HR face. HR version is an adaptive process for fusing the local pixel structure of diverse example faces to reduce the pressure of warping errors but does not recover the signals.

CONCLUSION

Replica based Image Reconstruction mechanism performs well with fMRI Data Set. The reconstructions were generated from the acquired magnitude fMRI images. The Replica based Image Reconstruction mechanism makes assumptions regarding the aliasing of the images and, hence, uses non-cartesian space sampling to spiral sampling conversion strategies. RIR presents reconstruction results using both Cartesian and spiral sampling strategies. Cartesian and spiral sampling strategies uses fMRI Set image from a real acquisition to improved dimensionality signal in the spatial domain. The RIR mechanism exact on high sparse image, improves SNR and image dimensionality. Theoretical analysis and experimental image results show that, algorithms applied on sparse space data improved SNR for effective analytical connection result. The experimental result of RIR mechanism attains minimal execution time, Noisy area in SNR, averagely 5.857% maximal accuracy rate, decreased computational complexity, least mean relative error and image dimensionality enhancement.

REFERENCES

Afonso, M.V., J.M. Bioucas-Dias and M.A.T. Figueired, 2011. An augmented lagrangian approach to the constrained optimization formulation of imaging inverse problems. IEEE T. Image Process., 20(3): 681-695.

Argyriou, V., 2011. Sub-hexagonal phase correlation for motion estimation. IEEE T. Image Process., 20(1): 110-120.

Averbuch, A., G. Lifschitz and Y. Shkolnisky, 2011. Accelerating x-ray data collection using pyramid beam ray casting geometries. IEEE T. Image Process., 20(2): 523-533.

Babacan, S.D., R. Molina and A.K. Katsaggelos, 2011. Variational bayesian super resolution. IEEE T. Image Process., 20(4):984-999.

Chen, B., H. Shu, H. Zhang, G. Coatrieux, L. Luo and J.L. Coatrieux, 2011. Combined invariants to similarity transformation and to blur using orthogonal Zernike moments. IEEE T. Image Process., 20(2): 345-360.

Chouzenoux, E., J. Idier and S. Moussaoui, 2011. A majorize-minimize strategy for subspace optimization applied to image restoration. IEEE T. Image Process., 20(6): 1517-1528.

Gajjar, P.P. and M.V. Joshi, 2010. New learning based super-resolution: Use of DWT and IGMRF prior. IEEE T. Image Process., 19(5): 1201-1213.

Giannoula, A., 2011. Classification-based adaptive filtering for multiframe blind image restoration. IEEE T. Image Process., 20(2): 382-390.

Hu, Y., K.M. Lam, G. Qiu and T. Shen, 2011. From local pixel structure to global image super-resolution: A new face hallucination framework. IEEE T. Image Process., 20(2): 433-445.

Hua, G. and O.G. Guleryuz, 2011. Spatial Sparsity-Induced Prediction (SIP) for images and video: A simple way to reject structured interference. IEEE T. Image Process., 20(4): 889-909.

Katsuki, T., A. Torii and M. Inoue, 2012. Posterior mean super-resolution with a causal Gaussian Markov random field prior. IEEE T. Image Process., 21(7): 3182-3193.

Koo, H.I. and N.I. Cho, 2011. Design of interchannel mrf model for probabilistic multichannel image processing. IEEE T. Image Process., 20(3): 601-611.

Lefkimmiatis, S., A. Bourquard and M. Unser, 2011. Hessian-based norm regularization for image restoration with biomedical applications. IEEE T. Image Process., 21(3): 983-995.

Li, X., 2011. Fine-granularity and spatially-adaptive regularization for projection-based image deblurring. IEEE T. Image Process., 20(4): 971-983.

Liao, H. and M.K. Ng, 2011. Blind deconvolution using generalized cross-validation approach to regularization parameter estimation. IEEE T. Image Process., 20(3): 670-680.

McEwen, J.D., G. Puy, J.P. Thiran, P. Vandergheynst, D. Van De Ville and Y. Wiaux, 2013. Sparse image reconstruction on the sphere: Implications of a new sampling theorem. IEEE T. Image Process., 22(6).

Montefusco, L.B., D. Lazzaro and S. Papi, 2011. Fast sparse image reconstruction using adaptive nonlinear filtering. IEEE T. Image Process., 20(2): 534-544.

Shaked, E. and O. Michailovich, 2011. Iterative shrinkage approach to restoration of optical imagery. IEEE T. Image Process., 20(2): 405-416.

Shi, G., D. Gao, X. Song, X. Xie, X. Chen and D. Liu, 2011. High-resolution imaging via moving random exposure and its simulation. IEEE T. Image Process., 20(1): 276-282.

Woolfe, F., M. Gerdes, M. Bello, X. Tao and A. Can, 2011. Autofluorescence removal by non-negative matrix factorization. IEEE T. Image Process., 20(4): 1085-1093.